TRANSPORTATION POOLED FUND PROGRAM
QUARTERLY PROGRESS REPORT

Lead Agency (FHWA or State DOT): ____Kansas DOT_____

INSTRUCTIONS:

Project Managers and/or research project investigators should complete a quarterly progress report for each calendar quarter during which the projects are active. Please provide a project schedule status of the research activities tied to each task that is defined in the proposal; a percentage completion of each task; a concise discussion (2 or 3 sentences) of the current status, including accomplishments and problems encountered, if any. List all tasks, even if no work was done during this period.

Transportation Pooled Fund Program Project # **TPF-5(328)**	**Transportation Pooled Fund Program - Report Period:** ☒Quarter 1 (January 1 – March 31) ☐Quarter 2 (April 1 – June 30) ☐Quarter 3 (July 1 – September 30) ☐Quarter 4 (October 1 – December 31)
Project Title: Strain-based Fatigue Crack Monitoring of Steel Bridges using Wireless Elastomeric Skin Sensors	
Project Manager: **Susan Barker, P.E.** **Phone:** **(785) 291-3847** **E-mail: SusanB@ksdot.org**	
Project Investigator: **Li Jian** **Phone:** **785-864-6850** **E-mail:** **jianli@ku.edu**	

Lead Agency Project ID: **RE-0699-01**	**Other Project ID (i.e., contract #):**	**Project Start Date:** **9/2015**
Original Project End Date: **Multi-year project**	**Current Project End Date:** **8/31/2018**	**Number of Extensions:** **N.A.**

Project schedule status:

☒ On schedule ☐ On revised schedule ☐ Ahead of schedule ☐ Behind schedule

Overall Project Statistics:

Total Project Budget	Total Cost to Date for Project	Total Percentage of Work Completed
$405,000	**$ 156,476.43**	**% 48**

Quarterly Project Statistics:

Total Project Expenses This Quarter	Total Amount of Funds Expended This Quarter	Percentage of Work Completed This Quarter
$ 33,890.64	**$ 33,890.64**	**8 %**

Project Description:
The main objective of this proposed research is to *provide state DOTs a practical and cost-effective long-term fatigue crack monitoring methodology using* ***a wireless elastomeric skin sensor network****.* This research is intended to demonstrate the value-added of fatigue crack monitoring of steel bridges using wireless skin sensors over the traditional bridge inspection.

Progress this Quarter (includes meetings, work plan status, contract status, significant progress, etc.):

ISU Progress:
Under this task, fatigue crack sensors are to be produced with an approximate thickness of 100-200 μm to enhance the mechanical robustness under harsh environment. Acceptable ranges of capacitance is 800-1000 pF. The anticipated number of sensors is 150 to 200 for the duration of the project.
A meeting occurred on October 7th during which it was agreed to start fabricating a different geometry (1'' x 1''). A total of 45 additional sensors have been delivered during this quarter. Technical support (Task 3) is being provided to KU on a continuous basis, as well as discussion and feedback (Task 4).

KU Progress:
KU team performed two tasks this quarter: finishing the threshold test and preliminary investigation of crack monitoring strategies for distortion-induced fatigue cracks.

UA Progress:
Arizona team has been focused on integrating the developed capacitive strain sensor board with the wireless sensor platform, Xnode. In particular, performance of the sensor board was evaluated under different power supply such as 5V and 3.2V. The Xnode supplies 3.2V directly to sensor board. 5V supply also can be used, but it requires a separate 5V power supply module and leads to less power efficiency. Under 5V supply, the sensor board showed good performance and measures strain levels as low as 30 micro strain. Under 3.2V supply, less effective performance has been observed; which may be attributed to the smaller balancing range than 5V supply, leading to higher noise. The sensor board is being modified to be connected with the Xnode. The measurement range of Xnode is 0V to 2.4V, so the output voltage of the sensor board needs to be within this range. For this reason, an additional amplifier and DC level controller was added to the board to adjust output voltage range.

Anticipated work next quarter:

ISU: Sensor production will continue in the next quarter. Technical support is being provided to KU on a continuous basis, as well as discussion and feedback.

KU: KU will finalize the numerical analysis of the distortion-induced fatigue detail within the bridge subassemblage model. Experimental test will be performed using the SEC sensor will be conducted to evaluate the crack monitoring performance of the SEC for distortion-induced fatigue cracks.

UA: In the next quarter, Arizona team will continue to focus on performance evaluation of the senor board and integration with the Xnode.

Significant Results:

Part 1: Crack detection using the SEC sensor

The KU team performed two tasks this quarter: finishing the threshold test and preliminary investigation of crack monitoring strategies for distortion-induced fatigue cracks.

1. Threshold test

In the last quarter, we conducted the threshold test using the steel compact specimen (Fig. 1). In the last quarterly report, the crack stopped growing at 1-1/2 in. when the load range was below the threshold of the fatigue crack growth. In this quarter, we resumed the crack growth by gradually increasing the load range to achieve a higher range of stress intensity factor ΔK, in order to evaluate whether the sensor was able to detect the resumed crack growth.

The threshold test has been finished in this quarter and the crack ultimately reached 1-15/16 in. The data in the threshold test is processed using the same data processing algorithm as previous tests. In the algorithm, the crack growth index (CGI) is proposed as a robust indicator for fatigue crack growth monitoring. Results of the threshold test are summarized in Fig. 2 and Fig. 3.

Fig. 2 shows the relationship between CGI and crack length and the applied ΔK vs. crack length. Between the two vertical dashed lines, the data points are collected when the ΔK is around the threshold for crack growth. As shown in Fig. 3, about 3 million cycles were applied and the crack pretty much remained dormant except that we observed very slight increase of length by 1/16 in. towards the end. The sensor reading also remained constant during this dormant period. After we increased the ΔK, as indicated in the data points beyond the second vertical line, the SEC sensor was able to produce increased CGIs when the crack reached longer length, indicating the ability of the SEC for crack monitoring during the second-phase crack growth.

Fig. 1. Test setup

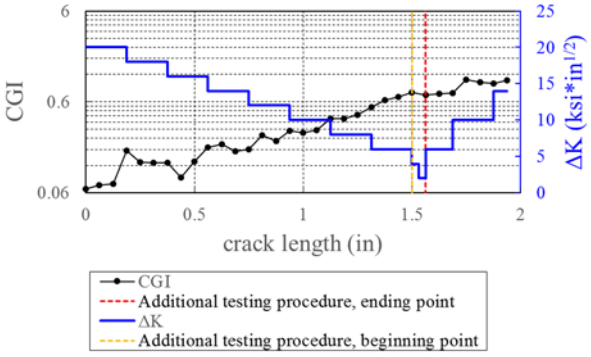

Fig. 2. Loading protocol of the threshold test

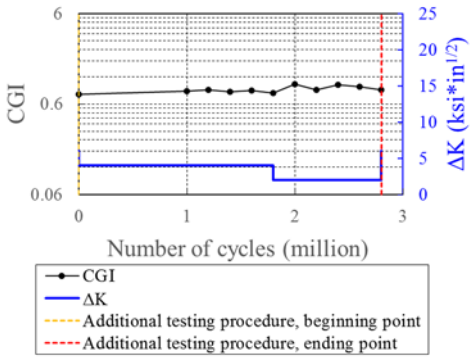

Fig. 3. Loading procedure at threshold ΔK

2. Preliminary analysis on distortion-induced fatigue crack in a reduced-scale bridge girder subassemblage model

Our next focus is to investigate the SEC's performance on a larger steel structure featured by its distortion-induced fatigue cracks. Fig. 4 shows the test setup of the bridge girder subassemblage model. In the setup, a W-shape steel girder is fixed on the strong floor. A steel cross-frame is connected to the girder web through a stiffener plate. On the other side of the stiffener, an actuator is attached to apply a vertical load. Instead of in-plane fatigue cracks investigated in our previous compact specimens, out-of-plane distortion-induced fatigue cracks have been generated in a few locations between the stiffener and the girder web. These cracks orient vertically, at the top and bottom of the stiffener on both north and south sides. The goal of this test is to investigate the crack monitoring ability of SECs for out-of-plane distortion-induced fatigue cracks.

Fig. 4. Test setup of the reduced-scale bridge girder subassemblage model

Compared with the previous compact specimens, one distinct feature of the bridge girder model is that fatigue cracks are caused by out-of-plane distortion between the cross frame and the web. Much higher strain concentrates around the crack region, and the strain field is highly related with the crack growth.

To investigate the strain field caused by cracking, finite element (FE) analysis is performed for the bridge girder model. The FE model is created with shell elements as shown in Fig. 5. To be able to numerically predict the SEC's response, a 2.5 in. by 2.5 in. region is selected at the bottom of the girder (Fig. 5) as the location of the sensor. In this case, the SEC would be folded 90 degrees for monitoring the crack growth at the corner. Two additional FE models (Fig. 6 and Fig. 7) are created, in which 1 in. crack and 2 in. crack are simulated by deleting elements.

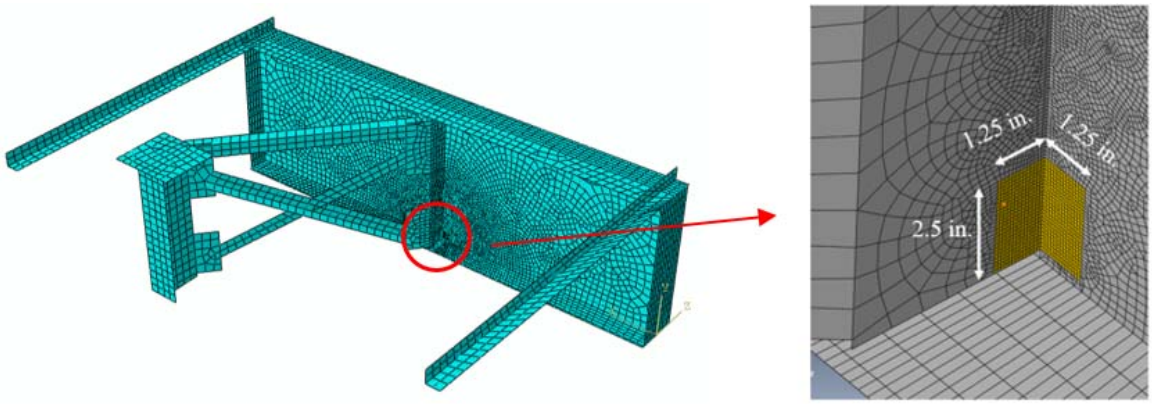

Fig. 5. FE model of the bridge girder subassemblage

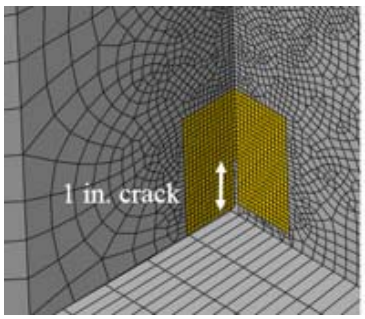

Fig. 6. FE model with a 1 in. crack

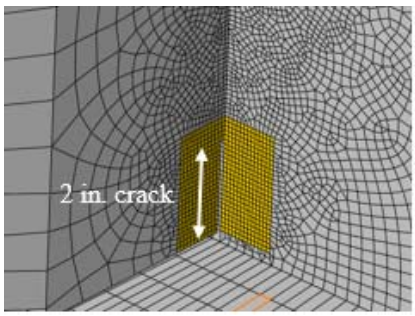

Fig. 7. FE model with a 2 in. crack

Fig. 8 shows the strain distributions of the uncracked model, model with1 in. crack, and model with 2 in. crack, respectively. As shown in the 2nd column of Fig. 8, large magnitude of strain can be found at the adjacent region of the crack path. In addition, when the crack propagates further, the concentrated strain field moves along with the crack tip. These findings indicate that the strain field under the SEC sensor changes dramatically when the crack grows.

The SEC's responses are numerically estimated by converting the strain results over sensor-covered region into capacitance. A numerical algorithm described in a previous quarterly report is utilized. Table 1 summarizes the estimated capacitance of the SEC contributed purely from the strain field on steel surface, hence does not include the capacitance caused by crack opening.

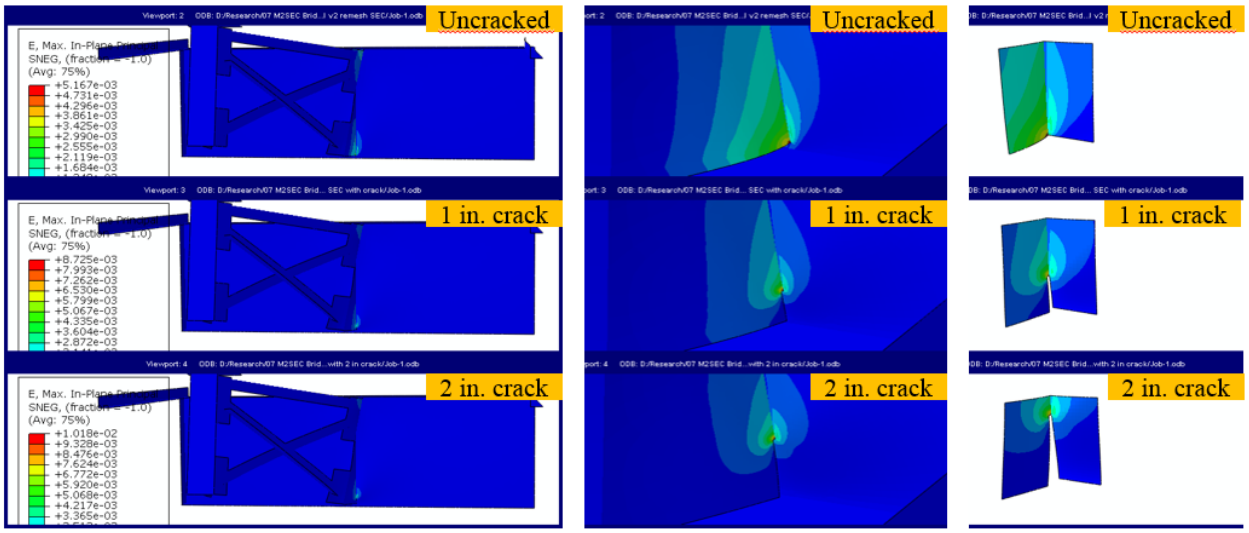

Fig. 8. Strain result of FE analysis: 1st column shows interior side of the steel girder; 2nd column shows the detail between the stiffener and the girder's web; and 3rd column shows the strain within the sensor area.

Two preliminary conclusions can be drawn from Table 1: 1) compared with previous tests using compact specimens, a much higher SEC's response (2.58 pF) is observed from the uncracked FE model; 2) when the crack propagates further, the concentrated strain field moves away from the sensor region, causing a lower SEC response. These preliminary findings will be utilized to create the testing plan.

Table 1. Estimated SEC response under different crack lengths

Name of the FE model	Estimated peak-to-peak capacitance (pF)
Uncracked FE model	2.58
Model with a 1 in. crack	2.49
Model with a 2 in. crack	1.68

Meanwhile, in preparing the experimental test, we have conducted a few tests to practice the installation of the SEC on complex structures surfaces such as around the corner between the web and stiffener. Fig. 9 shows the test setup. Two large SECs with dimensions of 3 in. by 3 in. are installed on the bridge girder. SEC #1 is attached on the flat surface of the top flange, while SEC #2 is folded 90 degrees and attached between the girder web and flange. Installation of SEC #2 is similar to the proposed testing plan where the SEC is attached between the stiffener and web for monitoring the vertical fatigue crack. A 0.5 Hz sinusoid load with peak-to-peak amplitude of 2.5 Kip are applied to the girder through the cross frame.

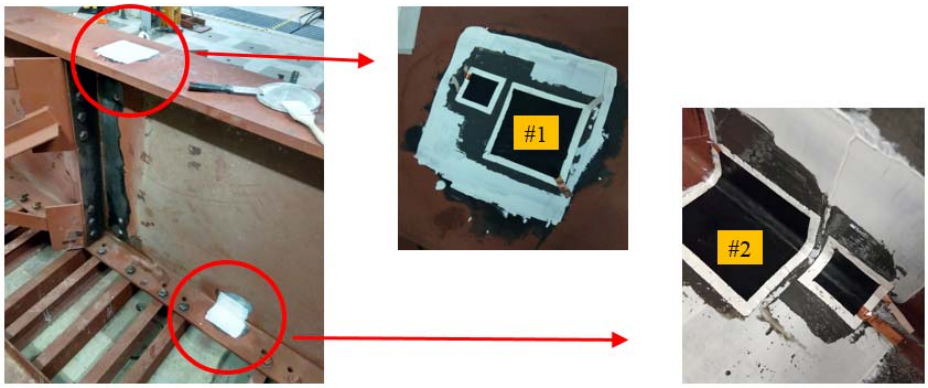

Fig. 9. Test setup

A 3-min measurement is taken during the test. Fig. 10 and Fig. 11 show typical SEC's responses in a 10 sec period. Fig. 12 shows the power spectrum density (PSD) of these two measurement, in which both SECs exhibit peaks around the loading rate (0.5 Hz). The result indicates the proper functionality of two SECs in terms of strain detection.

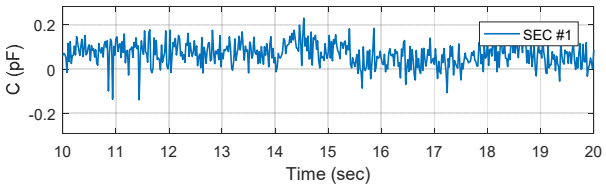

Fig. 10. Response of SEC #1

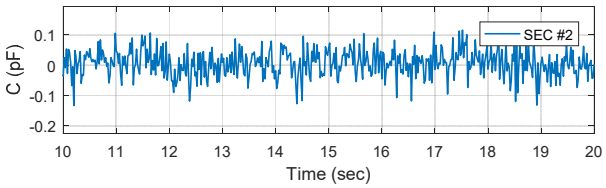

Fig. 11. Response of SEC #2

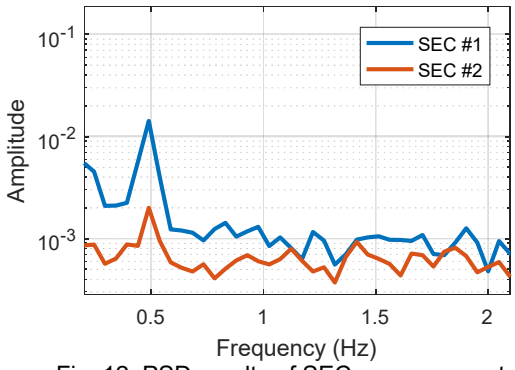

Fig. 12. PSD results of SEC measurement

Part 2: Wireless data acquisition

Large size (2.5inch x 2.5inch) SEC sensor performance was evaluated by dynamic shake table test under 2Hz sine wave. With 5V power supply, the sensor board clearly measured down to 30 micro strain level signal with the SEC sensor and showed linear relationship with foil type strain gauge measurement (Fig. 15). Test was done with 30 micro strain to 300 micro strain by increasing amplitude step by step. As shown in Fig. 15, SEC sensor showed clear sine wave that matches with strain gauge measurement.

Initially, the sensor board was designed to use 5V, because of easy development & testing. However, the Xnode wireless sensor platform provides 3.2V power supply for external sensors. Although the sensor board can still use 5V option with an additional power supply module, 3.2V directly from the Xnode is preferred as it is simpler. In addition, the output signals from the sensor board need to be adjusted within the sensing range of the Xnode (0V to 2.4V), corresponding board modification has been done in this quarter.

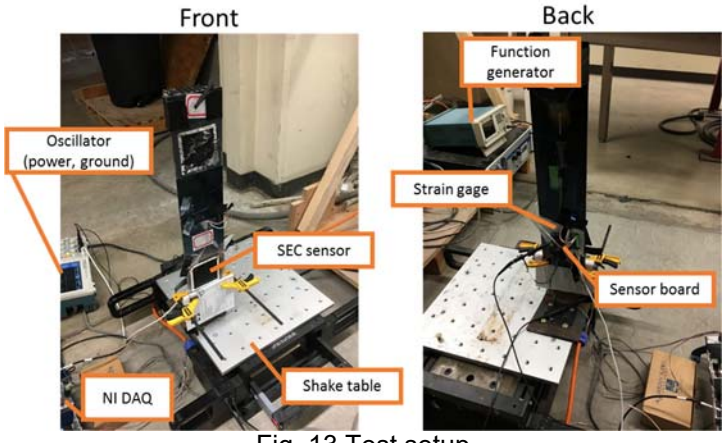

Fig. 13 Test setup

Fig.2 shows the picture of the new board and its schematic. A new amplifier (AD8226) is used to be compatible with the 3.2V supply. An additional amplifier has been added to control the final output voltage level. Since the Xnode sensing range is 0V to 2.4V, a new amplifier is needed to control DC bias voltage to fit the sensing range and provide additional amplification capability if necessary.

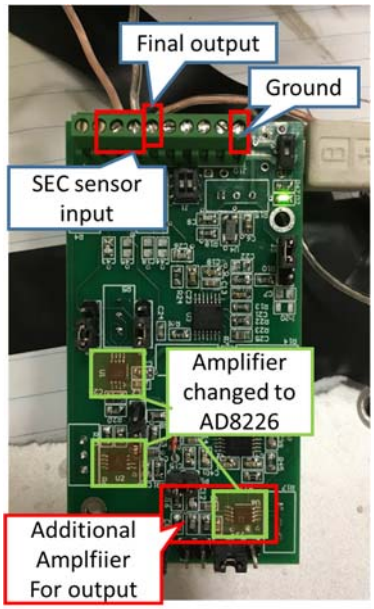

Fig. 14. New sensor board

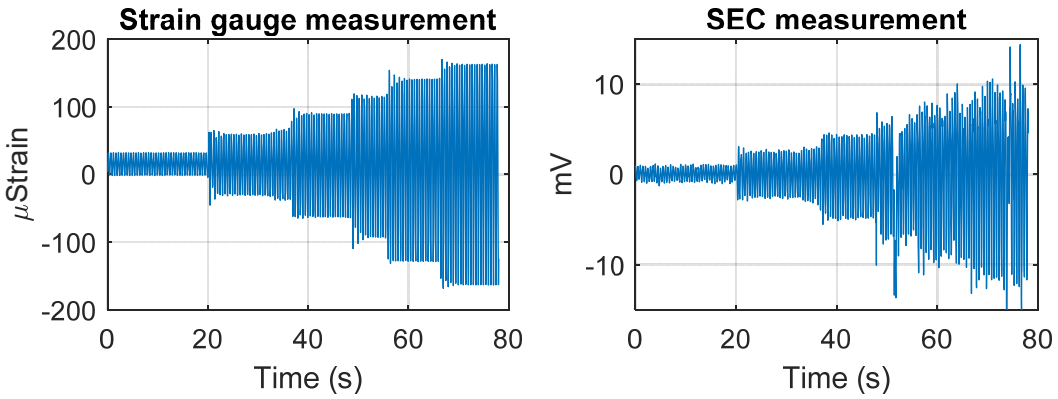

(a) Measurement comparison

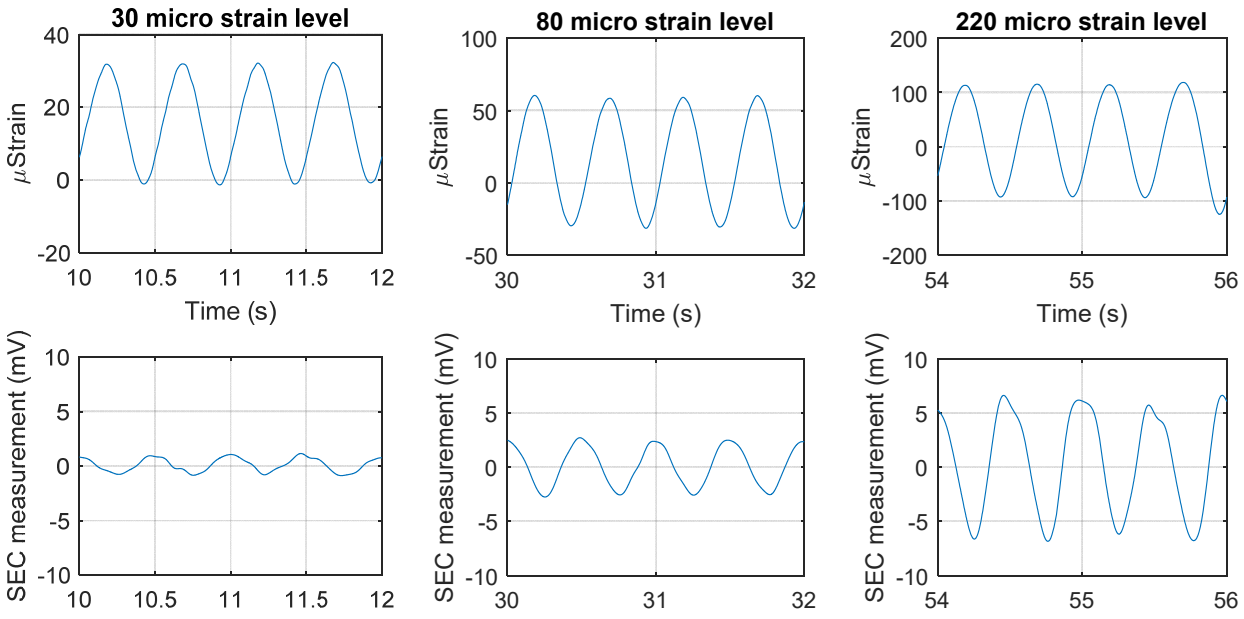

(b) Measurement comparision of each strain levels
Fig. 15. Dynamic Test Measurement (5V power supply)

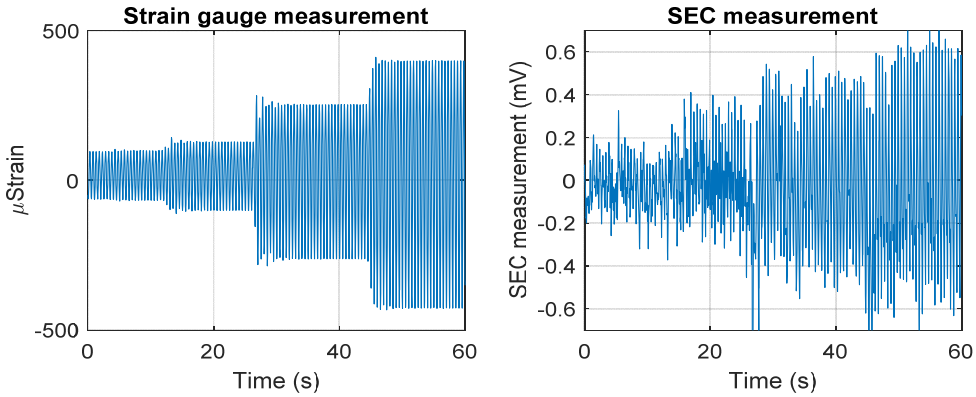

Fig. 16. Fig. 3 Dynamic Test Measurement (3.2V power supply)

Arizona team is currently evaluating the SEC sensor performance under 3.2V power supply and the interface with Xnode. Measurement under 3.2V supply tends to have more noise than the 5V setup (Fig. 16). In the next quarter, Arizona team will focus on improving sensor performance under 3.2V for direct use with Xnode.

The development of autonomous monitoring capability based on the Xnode platform has started. The KU team is in the process of getting the source code of the operating system for the Xnode, so that customization can be made to enable autonomous operation of the SEC sensor network for fatigue crack monitoring. Figure 17 shows the Xnode sensor platform and the software user interface for running sensing applications.

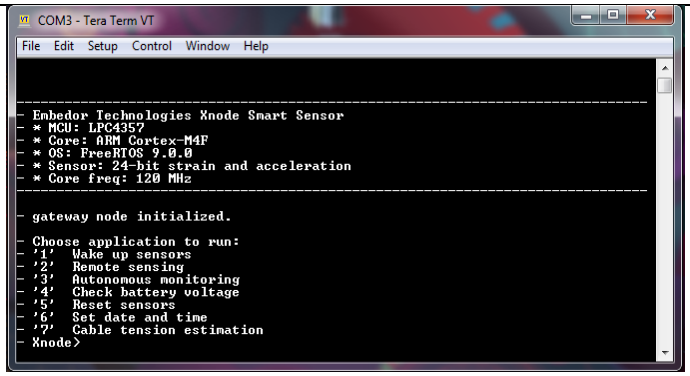

Figure 17. Xnode wireless sensor platform and the user interface

Circumstance affecting project or budget. (Please describe any challenges encountered or anticipated that might the completion of the project within the time, scope and fiscal constraints set forth in the agreement, along with recommended solutions to those problems).

None.